How to Reduce Refractory Spalling in Steam Reformer Furnaces

Operations improvements were developed by use of dynamic mathematical analyses of wide heat load variations and the resultant stress impacts on furnace tubes and walls.

C. McGreavy
Leeds University
and
M. W. Newman
Imperial Chemical Industries, Ltd.
London, England

Where steam reformers are used for production of town gas, the need to meet changing load demands means that the unsteady state performance of the furnance is of some importance. In particular, the permissible thermal stresses in the refractory walls and furnace tubes impose constraints that are especially significant when operating policy is established.

A dynamic model of an industrial furnace has been developed which has enabled an analysis of the refractory spalling problem to be made. Examination of the predictions in the light of plant data has enabled useful improvements in operating procedures to be developed.

Steam reforming process for manufactur of twon gas is an example of a plant which is subject to changes in load level at fairly frequent intervals. Consequently, for a significant part of the time, it operates under transient conditions, thus, some knowledge of the plant dynamics is obviously very important. In addition to providing information which can be used for the design of control systems, it makes it possible to identify when certain operating policies may result in the violation of process constraints. The concern here is with the latter problem.

Constraints on the system take many forms, but may be broadly categorized as either physical limitations of the processing equipment or restrictions on the product specification. Physical constraints arise on both the control and the process variables of the system: there is a maximum temperature that the furnace can attain; the flow rate of process gas through the tubes is restricted by the pressure drop through the catalyst bed; if the steam pressure is to be raised it has to be done slowly because of the finite capacity of the boilers. The latter problem, which is a dynamic constraint stipulating that the maximum rate of change of a variable must be within an overall limiting range of values, is of particular importance.

Constraints imposed on the dependent process variables are generally due to the mechanical strength of the equipment materials. The maximum pressure that the tubes can withstand is one obvious example. Again, dynamic constraints are particularly important here, as would arise, for example, for thermal shock effects in the furnace refractories and tubes when the burners are turned up or down.

It is this aspect that will be of primary interest in what follows, and it will be discussed with particular reference to the operation of the furnace in the Imperial Chemical Industries (ICI) process *(1)* using napatha as the feed.

The most important limitation

In practice, the most important limitation imposed on the furnace during non-steady state operation is concerned with the maximum thermal stresses that the refractory walls and furnace tubes can withstand. At the high working temperature of the metal, the calculated thermal stresses are indeed high if no allowance is made for stress relaxation induced by creep deformation of the material. In practice, however, the effects of creep are decisive. The creep rate is strongly temperature dependent, and also varies non-linearly with the imposed stresses, so that the resulting strain rates in different parts of the tube are complex functions of the heat flux variation. Moreover, it appears that the rate depends in some manner on the past history of the metal and is very difficult to explain in physical terms.

All that can be stated with confidence about the potential tube failure problem is that it is of a long-term nature *(2)*. For an immediate alteration in the load level or other operating conditions of the furnace, the refractory linings are far more susceptible to damage.

The problem of refractory spalling arises because of the non-uniformity of temperature within the slab. Under such conditions, free expansion of each volume element cannot occur because the elements are constrained to remain in the same body. The result is that stresses within the body are induced and these may eventually exceed the inherent mechanical strength of the material.

A linear temperature gradient does not give rise to thermal stresses because the body is able to expand without producing incompatible strains. A slab subjected to a linear temperature gradient will, if free to expand, form the arc of a circle in which each element of the slab has expanded by an amount proportional to its temperature increase. If the

temperature gradient is other than linear, however; there is no shape which the body can take up such that the expansion of each element is exactly satisfied. Instead, the body will assume a mean position such that some parts are in tension and the remainder in compression. Clearly the tensile and compressive stresses must balance one another.

In addition to these stresses there will be those due to the bending of the slab. If the temperature distribution were symmetrical about a plane through the mid-point of the slab thickness, the tensile and compressive stresses would likewise be symmetrical, and so no bending stresses could arise. In this case, however, the fact that one face is exposed to the hot furnace gases and the other to the external environment, gives rise to a mechanical couple about the mid-plane. They are balanced by bending stresses distributed over the cross section such that the algebraic sum of the moments of all bending forces is zero.

Prediction of the transient stresses which develop in the refractories requires information on the movement of the temperature profiles resulting from a change in the process operating conditions. Consequently, consideration must first be given to the formulation of a dynamic model of the furnace, so that this can be used in an analysis of the stresses developing in the refractories.

Dynamic model of the furnace

Furnace enclosure

A general schematic representation of the furnace used in the I.C.I. process is shown in Figure 1. The use of top-fired burners causes local turbulence which results in this region having an essentially uniform temperature. After flowing vertically down the furnace, the flue gases pass to a heat recovery section which generates steam for the process. Heat losses through the refractories forming the enclosure result in approximately linear temperature gradients within the pricks. Any disturbance which causes the heat flux within the furnace to alter will subject the refractory walls to transient changes in the temperature profiles, and this produces transient thermal stresses.

Assume that the furnace is essentially one-dimensional, with the distance variable defined along the length of the reactor tube. An overall differential energy balance gives

$$\rho_g C_g \frac{\partial Tg}{\partial \Theta} + \rho_g V_g Cg \frac{\partial Tg}{\partial Z} + \frac{\partial Hp}{\partial \Theta} + V_p \frac{\partial Hp}{\partial Z} + \frac{dO}{d\Theta} = 0 \qquad (1)$$

However, it is useful to de-couple the direct thermal effects of the gas streams by assuming that the flue gas is at a sufficiently high temperature that the heat flux to the reactor tubes is not influenced by the skin temperature of the tubes. Under these conditions the process gas can be regarded as a heat sink for the furnace. In these circumstances the two energy balances become, using the substantial derivative notation, $\frac{D}{D\Theta}$:

$$\frac{D}{D\Theta} H_g = \int_0^\infty (\beta_\lambda Q_\lambda - 4K_\lambda \sigma T_g^4) d_\lambda \qquad (2)$$

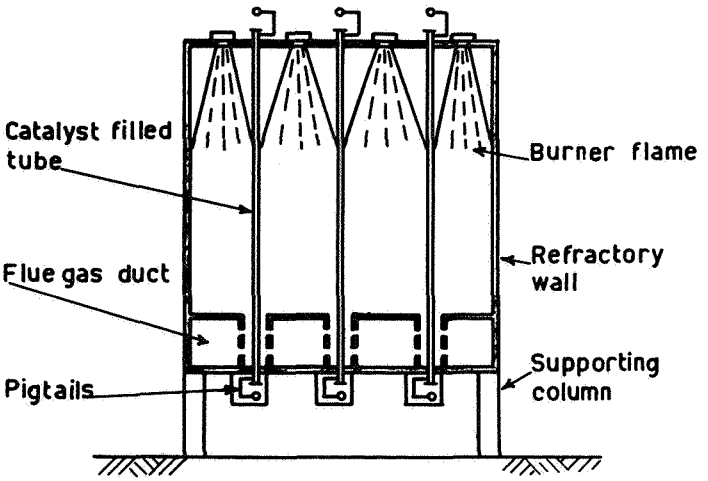

Figure 1. Schematic diagram of reformer.

$$\frac{D}{D\Theta} H_p = \int_0^\infty (a_t \epsilon_{t\lambda} - 2\sigma T_t^4) d_\lambda \qquad (3)$$

where the subscript λ refers to the monochromatic values and T_g and T_t are the flue gas and tube skin temperatures at time Θ and distance Z from the furnace roof.

The equations for the radiation flux, Q, are obtained by examining the energy distribution in more detail. Because the flux is expressed in terms of radiation beam intensities, the problem becomes that of obtaining manageable expressions for these variables. In turn, the intensities depend on the radiation emission and absorption functions. Simplification of the general equations is possible by:

(1) Using a directional average of flux intensity.

(2) Using a lumped approximation for the radiant heat source terms.

(3) Taking advantage of the band absorption-emission characteristics of the flue gases.

Average beam intensities

The rigorous expression for the beam intensities up and down the furnace involve both distance and angular variables. It is assumed that a mean angular flux can be defined which will only be a function of Z and will be denoted by I^+, I^-.

Radiant heat source terms

The basic assumption made in the present treatment is that in passing through each incremental volume of the furnace, the radiation beams will be attenuated by an amount proportional to the absorbing power of the flue gas, furnace tube surface, and refractory surface within that increment. In addition, the beams will be augmented by emission terms dependent upon the emissive powers and local temperatures of three materials within the same increment. This means that instead of integrating the source term over a finite path lenght, the mean value of the emission at a given horizontal level is taken as the sum of the individual terms for the gas, tube and refractory surfaces at that level.

Spectral energy distribution

Since the flue gases only tend to emit and absorb radiation in certain discrete bands, the spectral distribution can

be split into two groups representing absorption and transmission bands. Consequently, the total radiation flux can be approximated by an expression of the form:

$$I_a^+ + I_a^- + I_b^+ + I_b^- \qquad (4)$$

The subscript a refers to the absorption band and b the transmission band; the superscript $^+$ denotes the flux in the positive direction and $^-$ the flux in the negative direction. Details of the development may be found in reference *(3)*.

With these assumptions, the furnace equations take the form:

$$\frac{GgCg}{Vg}\frac{\partial Tg}{\partial \Theta} + GgCg\frac{\partial Tg}{\partial \Theta} = 2\beta\sigma\psi Tg^4 + \beta I_a^+ + \beta I_a^- \qquad (5)$$

$$\frac{\partial I_a^+}{\partial Z} = (-\beta - \epsilon_r a_r - \epsilon_t a_t)I_a^+ + \beta\sigma\psi T_g^4 + \epsilon_t a_t \sigma\psi T_t^4 + \epsilon_r a_r \sigma\psi T_r^4 \qquad (6)$$

$$-\frac{\partial I_a^+}{\partial Z} = (-\beta - \epsilon_r a_r - \epsilon_t a_t)I_a^- + \beta\sigma\psi T_g^4 + \epsilon_t a_t \sigma\psi T_t^4 + \epsilon_r a_r \sigma\psi T_r^4 \qquad (7)$$

$$\frac{\partial I_b^+}{\partial Z} = (-\epsilon_r a_r - \epsilon_t a_t)I_b^+ + \epsilon_t a_t(1-\psi)\sigma T_t^4 + \epsilon_r a_r(1-\psi)\sigma T_t^4 \qquad (8)$$

$$-\frac{\partial I_b^+}{\partial Z} = (-\epsilon_r a_r - \epsilon_t a_t)I_b^- + \epsilon_t a_t(1-\psi)\sigma T_t^4 + \epsilon_r a_r(1-\psi)\sigma T_r^4 \qquad (9)$$

$$\frac{1}{V_p}\frac{\partial Hp}{\partial \Theta} + \frac{\partial Hp}{\partial Z} = \epsilon_t a_t(I_a^+ + I_a^- + I_b^+ + I_b^- - 2\sigma T_t^4) \qquad (10)$$

The only variables which are considered to have time dependencies are the enthalpies of the flue and process gas streams. Clearly, however, the major lags in the system are due to the heat capacities of the solid components of the furnace; in particular, the influence of the refractory walls.

If the furnace burners are turned up, the new flame temperature consistent with the changed air-to-fuel ratio will be attained almost immediately. Likewise, the whole volume of flue gas will undergo a sudden temperature jump because the high flow rate causes the increased heat content of the gas in the vicinity of the flame to be rapidly carried to the lower section of the furnace. This will produce an instantaneous increase in the radiation heat flux emitted by the gas and falling on the refractory and tube surfaces; the rise in radiant flux, of course, being proportionally greater than the flue gas temperature increase.

Since the surface temperatures of the refractory and tubes do not change immediately, the flux the emit will be initially unaltered. Hence the surfaces absorb more radiant flux than they emit, with a consequent gradual increase in temperature until a new steady state is attained. The excess heat will gradually be conducted through the thicknesses of the refractory slab and tube walls, thereby bringing the interior temperatures (including that of the process gas and catalyst pellets), up to a new steady state.

Basically, therefore, the thermal lags in the system are the result of the material components acting as additional heat sinks, so that the full increase of available radiant heat cannot be realized immediately. Conversely, when the burners are turned down, the various component heat capacities act as additional heat sources, which prevent the radiant flux from falling immediately to its new steady state level of intensity.

Process gas side lags

The subsidiary partial differential equations describing the imbalance of heat in different parts of the furnace are derived by methods identical to those used for the original state equations. That is, the substantial derivative of the enthalpy of a component, which represents the accumulation of heat within unit volume during unit time, is equated to an energy balance between itself and other external components. Equation 5, for the flue gas, is already in this form, although, as stated above, its capacity term is negligible, and may be safely ignored.

Inside the furnace tubes, the process gas, catalyst pellets, and alloy steel tube walls all have finite thermal capacities, and should therefore be taken into account. An energy balance on the tube walls gives:

$$a_w \rho_t C_t \frac{\partial T_t}{\partial \Theta} = 2a_t h_{FW}(T_p - T_t) + \epsilon_t a_t(I_a^+ + I_a^- + I_b^- - 2\sigma T_t^4) \qquad (11)$$

For the fluid phase (process gas) the energy balance is:

$$\delta\rho_p C_p \frac{\partial Tp}{\partial \Theta} + \rho_p C_p V_p \frac{\partial Tp}{\partial \Theta} = 2a_t h_{FW}(T_t - T_p) + a_s h_{FC}(T_s - T_p) - Gp(\triangle H)/L \qquad (12)$$

Finally, the equation for the catalyst packing is:

$$(1-\delta)\rho_s C_s \frac{\partial T_s}{\partial \Theta} = a_s h_{FC}(T_s - T_p) \qquad (13)$$

In developing the above equations for thermal lags on the process gas side of the reformer, it has been assumed that gradients of temperatures and fluid momentum in a horizontal direction are absent. Axial diffusion of heat in the fluid is disregarded; so also is conduction along the tube length, or between vertically adjacent pellets. The net result of these simplifying assumptions is that the only spatial temperature distribution needing consideration is that of the process gas down the length of the tubes. This gives rise to the term for the bulk flow of process gas, and represents the only important mode of heat transfer in the vertical direction.

Horizontal heat movement

Convection and radiation of heat horizontally through the tubes is defined by the various heat transfer coefficients which provide lumped parameter approximations to very complex situations. The quantity h_{FC} is the overall heat transfer coefficient and the fluid-to-particle coefficient h_{FC} is determined from j–factor correlations *(4)*. The various

areas for heat transfer corresponding to these coefficients are based on unit volume of the reformer. Thus:

$$a_w = \frac{A_w}{L.Af} \tag{14}$$

$$a_s = \frac{\partial}{d_s}(1-\delta)\ \frac{At}{Af} \tag{15}$$

Where A_w is the cross-sectional area of all the metal walls of the furnace tubes, and A_t the sum of the cross-sectional areas of the empty tubes.

Examination of Equations 11 to 13 reveals that they are coupled together and must be solved simultaneously. Furthermore, the system is non-linear because of the inclusion of the terms for endothermic reaction heat and tube-skin radiant omission. In principle, Equation 11 shows that the process gas side equations should also be solved in conjunction with those of the radiation field; but the latter are insensitive to changes in tube-skin temperature, so this coupling may safely be disregarded.

To complete the system description, the initial perturbations that give rise to subsequent dynamic operation must be specified. Usually, this takes the form of stating new values for the dependent variables at the origins of both distance and time coordinates. In this case, however, it is the radiant flux intensity and process gas flow rate that change, whereas the inlet temperatures remain constant. Also, the perturbations are distributed along the *s*-dimension, and do not both occur simultaneously.

When the furnace throughput is to be increased, the burners are first turned up; this quickly increases the flue gas exit temperature, and, after a short delay, the amount of steam produced in the flue gas waste heat boilers. After the pressure in the drum has built up sufficiently, the steam flow rate to the furnace can be increased. The naphtha flow rate is linked to this by an automatic ratio controller. Thus, with regard to Equations 11 to 13, the initial disturbance is due to step-changes in the beam intensities. Then, after a certain time-lag, the process gas flow rate parameters *Gp* and *Vp* are increased. It is assumed that the change of flow rate is also a step function, and that the gas is incompressible; which means that an alteration in *Vp* at the inlet ($s = o$) is instantly propagated to the lower regions ($s > o$) of the reactor tubes. The non-linear interactive nature of the process gas equations, together with the separate perturbation conditions, precludes solution by analytical methods. However, numerical solution by finite differences is not difficult. The new profiles for tube-skin temperatures can therefore be substituted back into the radiation equations to update the beam intensities.

Conduction within the refractory wall

When considering the refractory wall, it is apparent that neglecting temperature gradients in the horizontal direction—i.e. through the slab thickness—is a gross assumption to make. The inside face temperature is in excess of 900°C, falling to ambient temperature through a thickness of about 0.75 ft. Moreover, the thermal conductivity of the refractory material is low, so that the chief resistance to heat transfer occurs within the solid itself, rather than at the two faces. A realistic treatment must, therefore, take account of the lateral temperature distribution through the wall.

The equations governing the transient state of the refractory wall are the well-known one-dimensional heat conduction equations, together with a flux boundary condition on the inside face to couple it with the radiation field:

$$\rho_r C_r \frac{\partial v}{\partial \Theta} = K_r \frac{\partial_s^2}{\partial_s^2} \tag{16}$$

$$Q_r = K_r\left(\frac{\partial T_r}{\partial_s}\right)_s = I_r^{=} h_{ri}(T_g - T_r) + \frac{\epsilon_r}{2}(I_a^{+} + I_a^{-} + I_b^{+} + I_b^{-} - 2\sigma T_r^4) \tag{17}$$

where $v\ (s,G)$ is the temperature distribution through the slab thickness, and T_r the value of v at the inside face ($s = l_r$). In Equation 17, the term $(T_g - T_r)$ represents the flow of heat into the hot face by convection, which maintains the steady state temperature gradient. This amount of heat is eventually lost to the atmosphere from the outer face; thus the second boundary condition should be of the form:

$$K_r\left(\frac{\partial v}{\partial s}\right)_{s=o} = h_{ro}(v - T_A) \tag{18}$$

However, in practice, the flux at the outer refractory surface is negligible in the dynamic analysis of the furnace, hence, putting $h_{ro} = \infty$ this boundary condition becomes a prescribed surface temperature

$$v_{s=0} = I_A \tag{19}$$

The appropriate initial condition for the equations is the original steady-state temperature profile through the slab, given by:

$$v(s,0) = (T_r - T_A)\ \frac{s}{l_r} + T_A \tag{20}$$

There is a set of Equations, 16 to 20, applicable to each horizontal increment of the furnace. In the boundary condition at the inside face, the radiation beams and surface temperature are functions of *s*, the distance down the furnace, thus giving rise to varying amounts of radiant flux to be absorbed by the refractory. However, vertically adjacent sets of equations are not coupled because conduction of heat along the length of the refractory wall is neglected, hence they may all be solved independently.

The radiant flux to the refractory is not only a function of *s*; it is also strongly time-dependent. Immediately after the burners have been turned up, there is a large net flow of heat to the refractory, but as the surface temperature gradually rises, more flux is emitted and the amount potentially available to raise the temperature further is reduced. Eventually, the radiation field and refractory surface will once again be in a steady state. When this occurs, the furnace has, for most practical purposes, also reached its new steady state. The conduction equation will show that the interior of the refractory slab is still in a transient state, but this is of minor importance. Clearly, the major interest

is in the initial stages of the dynamic response of the furnace.

For a thermal conductivity independent of temperature and position, and neglecting conduction effects parallel to the surface of the refractory, the transient profiles for constant boundary conditions are *(5)*

$$v = 2\sqrt{a_r\Theta}\left(\frac{Q_r}{k_r} - \frac{T_r}{l_r} + \frac{T_A}{l_r}\right)\sum_{n=0}^{\infty}(-1)^n\left\{\text{i erfc}\,x_1 + \text{i erfc}\,x_2\right\} + \frac{(T_r - T_A)}{\rho_r}s + T_A \qquad (21)$$

where:
$$x_1 = \frac{(2n+1)l_r + s}{2\sqrt{a_r\Theta}} \qquad (22)$$

and:
$$x_2 = \frac{(2n+1)\rho_r - s}{2\sqrt{a_r\Theta}} \qquad (23)$$

The integrals of the complimentary error function for arguments x_1, x_2 is available from the standard mathematical tables.

Thus, at a particular horizontal level s, the temperature profile through the slab thickness may be denoted by $T_s(y, \Theta)$. The complete set of equations can be solved by computer, details of which can be found elsewhere *(3)*.

Stress analysis in the refractory walls

During a transient change in the temperature profiles in the refractory walls as a consequence of adjustment of the process conditions, stresses will be set up which can cause mechanical failure of the bricks.

The wall thickness is small compared with the overall dimensions of the furnace box so that stresses perpendicular to these planes can safely be neglected. In fact, they consist of many individual firebricks, approximately cubic in shape and covered with a layer of heat-resistant ceramic on the inside and insulating material on the outside. Consequently, the assumption of a homogeneous slab will give a conservative estimate of the ability of the refractories to withstand thermal shock. It can be easily shown that the thermal stresses at any point y within the slab is given by the expression *(6)*.

$$\sigma_{xx}(y,\Theta) = \frac{aE}{1-\gamma}\left[\frac{1}{\rho_r}\int_o^b T_g(y,\Theta)dy + \frac{12y}{\rho_r^3}\int_o^b T_g(y,\Theta)ydy - T_2\right] \qquad (24)$$

Solution of the dynamic equations provides the necessary temperature profile T_z for use in the above quadrature.

In a study of thermal shock tests for refractories Hasselman *(7)* has given general analytical solutions for the case of a suddenly applied constant heat flux. However, the calculated stresses for this treatment approach constant values as time approaches infinity and this is at variance with actual conditions where the stresses achieve maximum values then fall to zero when the slab temperature reaches a new steady state. Moreover, in the present case, the heat flux at the boundary is not constant.

For an arbitrary time variation of heat flux input, the temperature or stress profiles at time Θ may be obtained by the application of Duhamel's Theorem, which gives:

$$T_z(y,\Theta) = \int_o^t \frac{q(\tau)}{q^0}\frac{\partial T}{\partial\Theta}(y,\Theta-\tau)\,d\tau \qquad (25)$$

The superscript zero refers to the values applicable to a constant heat flux q^0 maintained over a time interval Θ. The variable τ can be regarded as a subdivision of Θ; i.e. $q(\tau)$ refers to the instantaneous value of heat input at time τ where $0 \leqslant \tau < \Theta$.

Integrating Equation 25 by parts gives:

$$T_g(y,\Theta) = \frac{q(0)}{q^0}T^0(y,\Theta) + \frac{1}{q^0}\int_o^t \frac{dq(\tau)}{d\tau}T^0(y,-\tau)\,d\tau \qquad (26)$$

The stress due to time-varying heat inputs can be obtained from σ_{xx}^0 (that due to constant q^0) by direct application of Duhamel's Theorem without first determining the temperature profile for the varying case. The equivalent equation for the stress is:

$$\sigma_{xx}(y,\Theta) = \frac{q(o)}{q^0}\sigma_{xx}(y,\Theta) + \frac{1}{q^0}\int_o^t \frac{dq(\tau)}{d\tau}\sigma_{xx}^0(y,\Theta-\tau)\,d\tau \qquad (27)$$

This equation shows clearly how the "history" of the thermal inputs experienced by the refractory slab influences the resultant stress. It is not sufficient merely to know the instantaneous distributions of q and τ because the rates of changes of these quantities have a vital bearing on the stress levels attained.

In principle, the stress analysis should be done at each horizontal increment down the furnace, but a severe limitation is the amount of computational effort required. Therefore, the slab stresses are only calculated for two horizontal levels—at the furnace roof and at the place in the wall opposite the burner flames, i.e. facing the hottest gas temperature.

Discussion

Tests on the dynamic model, and comparision with plant data have confirmed that it can reliably predict the behavior of the furnace *(3)*. There is, therefore, some confidence in using the computed temperature profiles in a stress analysis.

Some of the other inherent complexities of the problem and the simplifying assumptions made have been mentioned already. There are, however, several others in addition, and these may be conveniently considered now.

The maximum stresses calculated will be those necessary to initiate a fracture; whether or not propagation of the

crack with consequent spalling will occur is another problem. Griffith *(8)* describes a criterion for crack propagation based on the strain energy in unit volume of the material. However, Kingery *(9)* considers the value of those quantitative predictions questionable, and they have not been included here.

A further important assumption concerns the ommission of mechanical traction or body forces superimposed on the thermal stresses that arise. In this case the most important body force is the weight of the bricks and any loads that they bear. These induce compressive forces in the slab which, as shown later, are less important than tensile stresses.

Other assumptions include neglecting the effect of creep deformation, taking constant mechanical and thermal properties for all temperatures, and neglecting "end effects" at the corners of the slab. Regarding creep, a paper by Hasselman *(10)* defines a relaxation time for the stresses to decay by creep mechanisms. Based on typical grain sizes and other material properties for firebrick, it is found that at the temperature levels involved the relaxation time calculated is very long compared with the time during which the furnace undergoes state operation.

The material property values required for firebrick are set out in Table 1. The slab thickness indicated is for the roof and that part of the wall opposite the burner flames; further down the wall is thicker. An average temperature of 500°C was chosen at which to estimate the material properties.

Four cases are considered here. They all involve step changes in both burner fuel flow and make gas throughput of some 20% or more from the original steady state levels. The important input variables are summarized in Table 2. It is seen that Case 1 involves a step increase from minimum make; Case 2 is a step increase from normal make to essentially the maximum load; Case 3 is a step reduction from normal make; and Case 4 a step reduction from maximum to roughly normal make. The dynamic conditions for all these cases are substantially more severe than would arise in practice.

The general shape of the stress profiles for heating the slab is shown in Figure 2 (a). During the initial stages, the outer surfaces are under compressive stresses while the bulk of the inner core is in slight tension. The compressive stresses then reach their maxima on the wall surfaces (greatest on the hot face where the flux change is made) and the flat tensile stress curve becomes more peaked. Then the tensile stress achieves its maximum in the interior of the slab and the curve assumes the shape of a skewed parabola as shown in Figure 2 (a). The compressive stresses have

Table 1. Properties of the refractory walls

Slab thickness, inches	6.0
Young's Modulus, lb/sq.in	4.0×10^6
Poisson's Radio	.027
Thermal conductivity, CHU/hr/sq.ft./°C	840
Density, lb/cu.ft.	124
Specific heat, CHU/lb./°C	0.24
Emissivity	.080
Thermal expansion coefficient, $°\ C^{-3}$	4.5×10^{-6}
Ultimate tensile strength, lb./sq.in.	500
Crushing (compressive) strength, lb./sq.in.	4400

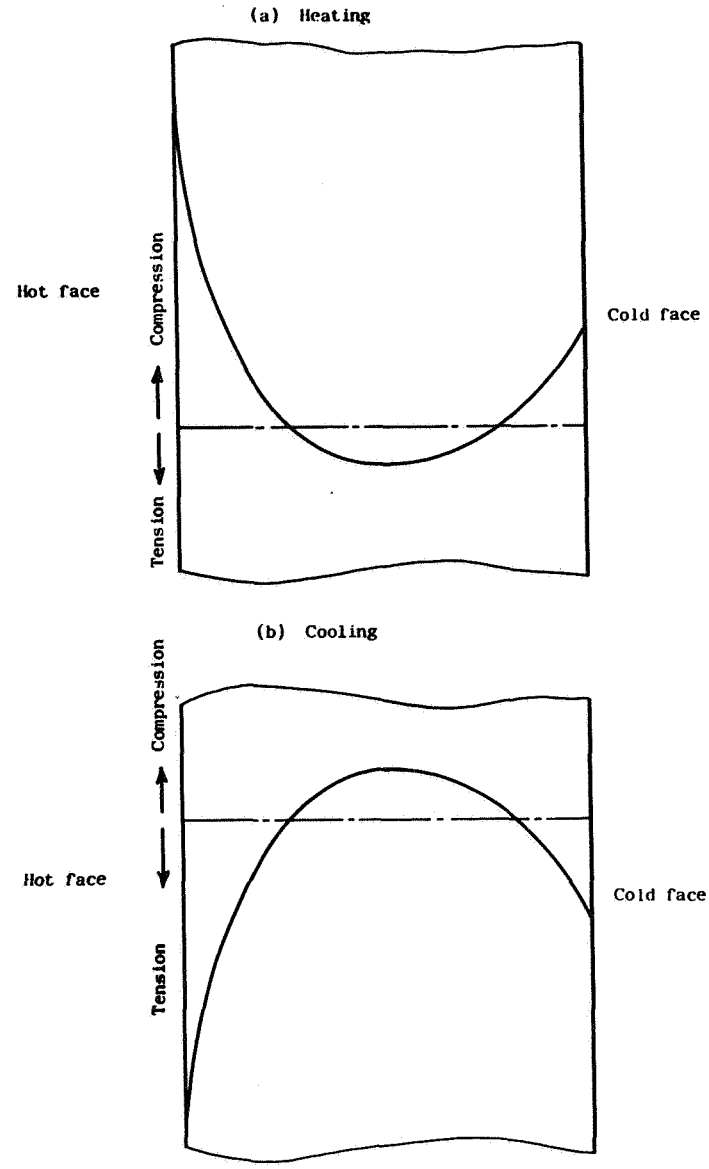

Figure 2. General shape of stress profiles through refractory slab; heating at (a) above; and cooling at (b) below.

Table 2. Input flow rates for stress analysis runs

Flow	Initial value	Final value
Case 1:		
Burner fuel	1,500	1,800
Combustion air	32,000	32,000
Process gas	22,000	26,400
Case 2:		
Burner fuel	2,600	3,100
Combusion air	54,000	54,000
Process gas	39,000	47,000
Case 3:		
Burner fuel	2,600	2,100
Combusion air	45,000	45,000
Process gas	39,000	31,000
Case 4:		
Burner fuel	3,200	2,500
Combusion air	57,000	57,000
Process gas	48,000	38,000

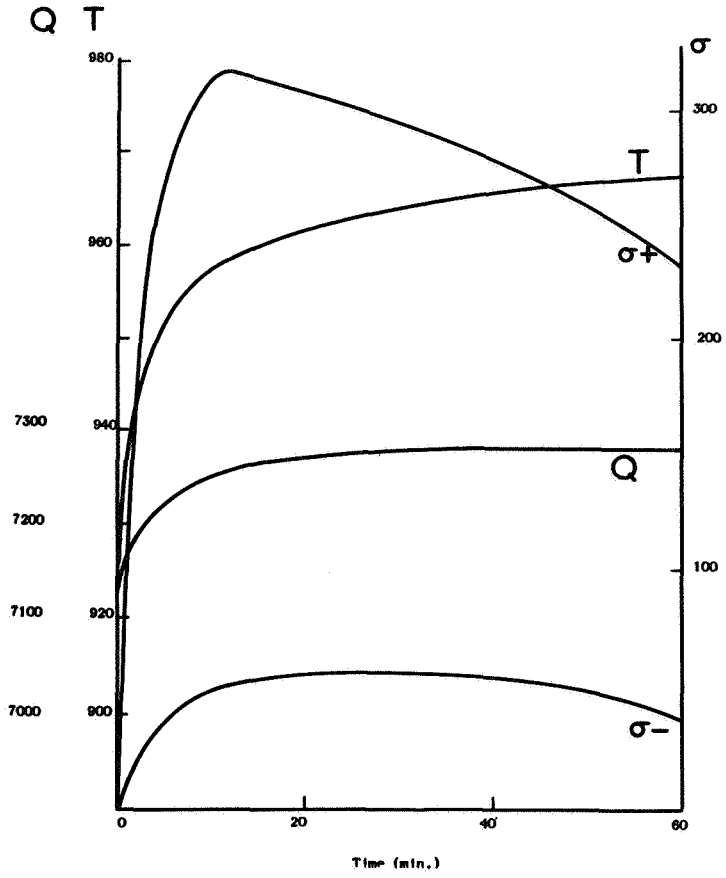

Figure 3. Heat flux, temperature, and maximum stress variation as a function of time for increase from minimum make.

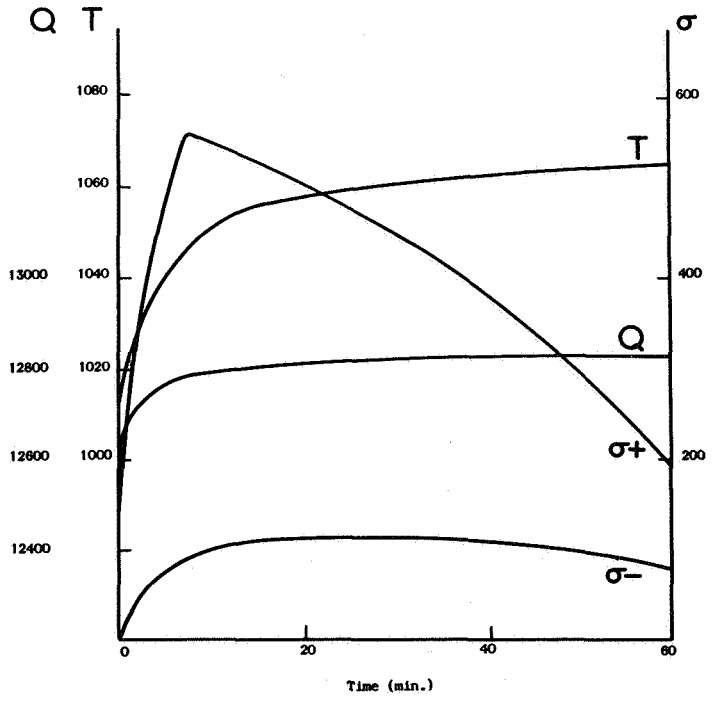

Figure 4. Heat flux, temperature, and maximum stress variation as a function of time for increase from normal make.

diminished. Finally, all the stresses will become zero again, although the computations are not pursued to this point.

When the refractory walls are cooled by reducing the load, the corresponding stress profiles are shown in Figure 2 (b). The pattern is similar to the heating case except that

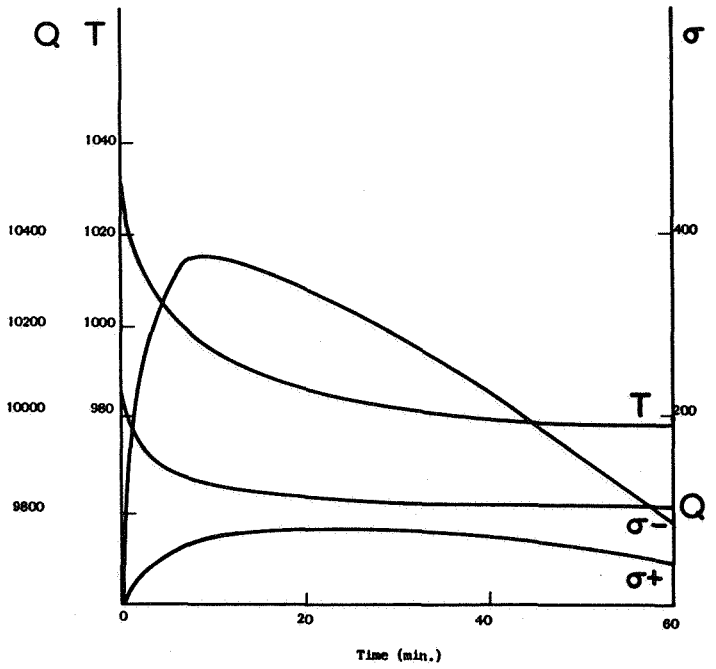

Figure 5. Heat flux, temperatures, and maximum stress variation as a function of time for reduction from normal make.

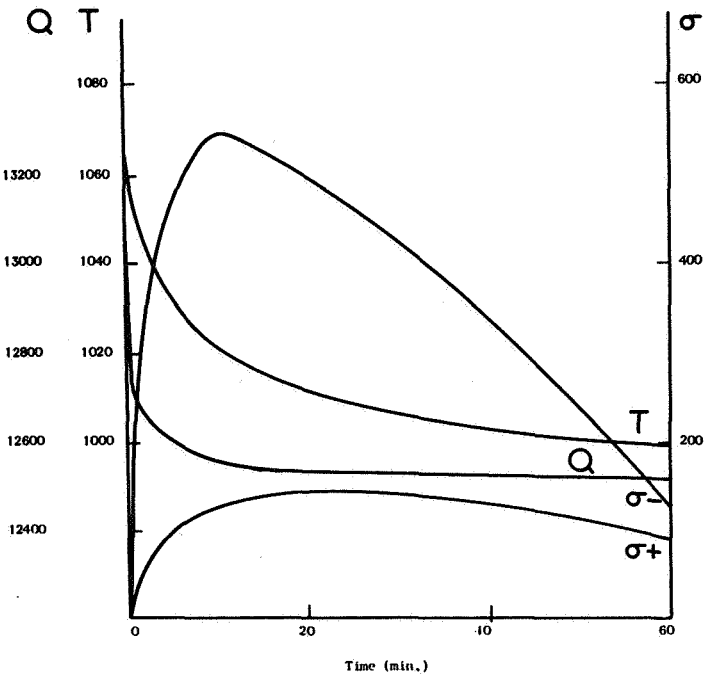

Figure 6. Heat flux, temperature, and maximum stress variation as a function of time for reduction from maximum make.

the tensile and compressive parts of the curve are interchanged. Also the profile is less skewed. Here the compressive stresses are of no interest because long before their maxima are reached the slab would have failed in tension.

The salient features of the results obtained from the four computer runs are presented in Figure 3 to 6. At each time step the values of the following variables are given: (a) inside wall temperature, T_r; (b) heat flux to wall, q_r; (c) maximum tensile stress, σ^-_{min}; and (d) maximum compressive stress σ^+_{max}.

The plant process operators are not allowed to raise the

load level at such a rate that the rise in flue gas exit temperature exceeds 50°C/hr. This is equivalent to a rise of about 38°C/hr. for the refractory temperature. The changes resulting from Cases 1 and 2 are equivalent to changes of 42°C and 61°C/hr. respectively in the maximum hot face refractory wall temperature, but the maximum tensile stresses induced never exceed 40% of the failure level. The compressive stresses are less than 20% of the maximum, even though the calculated compressive stresses are six times the tensile stresses. It would therefore appear that the safety margin is ample and the furnace load level could be increased more rapidly if the need arose. It might be truer to say that the problem of refractory spalling is not the limiting constraint when the load level is being increased.

When reducing the load, the program calculates that the ultimate tensile strength is exceeded when the rate of change of temperature is of the order of 65°C/hr. Thus when reducing the throughput, considerably more care must be taken because the margin of safety is very much less. Bearing in mind the assumptions made, this is nevertheless still a conservative estimate.

Conclusions

Using a dynamic model of a steam reforming furnace which has been shown to predict reliably the transient response of process, an analysis of the thermal shock characteristics has been carried out. It has been shown that the stress profiles are such that large stresses can be induced at the hot face of the wall during transient conditions. Since the mechanical strength of the refractory is order of magnitude greater in compression than in tension, this indicates that mechanical failure due to rapid heating is not likely to be a problem. On the other hand, quenching effects, such as might occur during plant shutdown are a far more serious consideration because the hot face is under tension. Normal operating practice for changes in load levels appears to work well within the capability of the refractory to withstand thermal shock.

Acknowledgments

Thanks are due to S.P.S. Andrew for helping discussions during this work and to NEGAS for access to their plant for testing of the models. #

Nomenclature

A_f = cross sectional area of furnace box.
A_t = total surface area of tubes.
A_w = total cross sectional area of tube metal wall.
a_t = half furnace tube surface area per unit volume.
C_p = process gas specific heat.
C_g = flue gas specific heat.
C_r = refractory specific heat.
C_s = catalyst pellet specific heat.
d_s = effective catalyst pellet diameter.
E = Young's modulus of elasticity for refractory slab.
H_p = enthalpy of process gas stream.
H_g = enthalpy of flue gas stream.
h_{FC} = overall catalyst pellet-process fluid heat transfer coefficient.
h_{FW} = overall tube skin-process fluid heat transfer coefficient, assuming absence of catalyst pellets.
h_{ri} = heat transfer coefficient between flue gas and refractory wall.
h_{re} = heat transfer coefficient between outside face of refractory.
I_a^+ = downward component of radiation intensity that interacts with furnace gas.
I_b^+ = upward component of radiation intensity that interacts with furnace gas.
I_a^- downward component of radiation intensity that does not interact with furnace gas.
I_b^- = upward component of radiation intensity that does not interact with furnace gas.
K_r = thermal conductivity of refractory slab.
L = total heated tube length.
ϵ = thickness of gas through which radiation beam passes.
ϵ_r = refractory slab thickness.
Q = radiation heat flux within furnace enclosure.
$q(\tau)$ = instantaneous heat flux to refractory walls at time.
q^0 = heat flux to refractory wall during time step in which the refractory slab temperature and stress distributions are evaluated.
R = gas constant.
T_p = temperature of process gas.
T_g = temperature of flue gas.
T_t = temperature of tube skin.
T_r = temperature of refractory hot face.
T_i = temperature that characterizes heat input to furnace.
T_A = ambient temperature.
T_Z = temperature at internal position within refractory slab.
V_g = velocity of flue gas.
V = temperature distribution through refractory slab wall.
$\frac{X_1}{X_2}$ = groups of terms defined by Equations 23 and 24.
χ = distance from source of beam propagation.
Z = distance down furnace (downward direction positive).
α = thermal expansion coefficient of refractory slab.
α_r = thermal diffusivity of refractory slab.
α_λ = fraction of monochromatic beam absorbed by gas.
β = volumetric absorption coefficient of flue gas.
δ = bed voidage fraction.

ϵ_p = emissivity of process gas.

ϵ_g = emissivity of flue gas.

ϵ_t = emissivity of tube wall.

ϵ_r = emissivity of refractory slab.

ϵ_s = emissivity of catalyst pellets.

ζ = net flux absorbed by refractory wall in unsteady state.

Θ = time increment.

θ = time variable.

κ = flue gas mass absorption coefficient.

ξ = Poisson's ratio for refractory wall.

ρ_p = density of process gas.

ρ_g = density of flue gas.

ρ_r = density of refractory wall.

ρ_s = density of catalyst pellets.

σ = Stefan-Boltzmann constant.

σ_{xx} = stress distribution in refractory wall.

Υ = continuous time variable into which discrete increment Θ is subdivided.

ψ = fraction of the spectrum that can absorb and emit radiation.

W = solid angle over which beam is propagated.

Literature cited

1. Andrew, S.P.S., *Chem. and Ind.* p. 826, (1965).
2. Ellis, J.F., Paper given at the Ann. Gen. Mtg. of the Soc. of Chem. Ind., 16th July 1964, Manchester, Eng.
3. McGreavy, C. and M.W. Newman–to be published.
4. Salterfield, C.N. "Mass Transfer in Heterogeneous Catalysis" M.I.T. Press (1970).
5. Carslaw, H.S. and Jaeger, J.C., "Conduction of Heat in Solids," 2nd Ed., Claredon Press, Oxford (1959).
6. Boley, B.A. and Weiner, G.H., "Theory of Thermal Stresses," Wiley (1960).
7. Hasselman, D.P.H., *J. Amer. Ceram. Soc.* **46**, 229 (1963).
8. Griffith, A.A., *Phil. Trans. Roy. Soc.* **A221**, 163 (1920).
9. Kingery, W.D., *J. Amer. Ceram. Soc.* **38**, 3 (1955).
10. Hasselman, D.P.H., *J. Amer. Ceram. Soc.* **50**, 454 (1967).